Validating the performance of a Raman laser spectrometer (RLS) instrument under Martian conditions

Motamedi Mohammadabadi, K.

2013

document version
Publisher's PDF, also known as Version of record

6.1 Performance of the RLS instrument under Martian conditions

The first objective of this PhD research was to design, manufacture and test a simulation chamber (MASC) to reproduce the atmospheric conditions of Mars. The MASC is a temperature and atmosphere controlled chamber (200 l). In order to reproduce Mars' atmosphere and temperature inside the MASC, an innovative heating-cooling system was coupled to a vacuum and gas control system (more details about the MASC chamber are found in chapter three). The MASC chamber can simulate planetary atmospheres and by doing so we are able to:

- Perform *in situ* sample analysis
- Test the performance of space instruments.

The second objective of this PhD research was to validate the performance of the RLS instrument within the MASC under Martian conditions, specifically assessing the capability to determine Raman spectra on minerals thought to be present on the Mars surface. Therefore, the RLS instrument was installed inside the MASC and the performance of the RLS instrument was evaluated and discussed in previous chapters.

This chapter reviews the performance of the RLS instrument under practical conditions and based on the performance makes recommendations for potential improvements for future mission instruments. A major observation of this work is that the RLS instrument is far less effective at producing and detecting Raman signals than the commercially available Renishaw InVia Raman microscope that we used for comparison studies. We evaluate key aspects of performance of the RLS EB instrument and make a series of suggestions for improvements for RLS instruments for future planetary missions.

Basic RLS instrument calibration: The performance was initially assessed based on the calibrations of the spectrometer at different temperatures. Visible light (~ 400– 800 nm) was directed at the RLS instrument to localise the position of the orders on the CCD (for this research, the 3rd order (660– 800 nm) was used for Raman analyses). The positions of the orders on the CCD were influenced by the temperature of the spectrometer. The result of the calibrations suggested that the prism of the RLS instrument was significantly affected by thermal changes.

Consequently a discussion of the role of the prism and grating in the RLS instrumentation design is warranted to understand how the prism and grating may influence RLS data obtained under Martian conditions. The prism in the RLS instrument was used to separate Raman emission light into its constituent spectral colours with their different range of wavelengths. Therefore, the spectrum of light is separated vertically by wavelengths. Then, the light with different ranges of wavelengths reaches a grating in the RLS instrument. Light with different wavelengths disperses from grating in different directions and creates diffraction orders (see section 2.4.3 for more information). Gradually lowering the temperature of the RLS instrument from 10 to -20 °C led to a vertical shift in the position of

the orders on the CCD of the spectrometer (~ 3 pixels or 40 μm). The most probable causes of the change in position on the CCD are:

- (Unwanted) movement of the prism
- (Unwanted) change(s) in the properties of the prism due to the thermal expansion

A key observation is that the makeup of the individual orders did not change and that all the wavelengths in each order remained the same. In addition, the orders did not shift horizontally on the CCD so that wavelength calibrations were not affected. From these observations we conclude that the grating was not affected by temperature. The CO_2 pressure (~ 8 mbar) had no effect on Raman spectra of this study (see chapter four and five). Consequently, we conclude that the RLS instrument can be operated under Martian atmospheric conditions where temperature can vary in the range +10 to -20 °C. The effect of temperature variation on the RLS instrument performance is fully characterised in chapter two, section 2.5.2.

The final objective of this PhD research was to assess the effectiveness of the RLS instrument in obtaining Raman spectra from different minerals under Martian conditions. Chapters four and five described that there was no influence of temperature and pressure on mineral Raman spectra at Martian conditions. Different composition in mineral structure caused frequency shifts.

6.2 Detection of minerals with the RLS instrument

A variety of different mineral compositions were successfully identified with the RLS instrument under Martian conditions. A list of analysed minerals is reported in table 6.1. These minerals were selected because they are already known or suspected to exist on Mars and identification of these minerals will help in understanding the evolution of planet Mars (see chapter one for more information). The minerals are classified in three groups, depending on the ability of the RLS instrument to detect them and the reason for the success or otherwise in detecting the minerals are discussed:

Group *A*: Minerals that were successfully identified
Group *B*: Minerals that were more difficult to detect
Group *C*: Minerals that were not identified

Minerals in group A and B	
A	**Sulphates:** - Barite ($BaSO_4$) - Anglesite ($PbSO_4$) - Gypsum ($CaSO_4 \cdot 2H_2O$) (hydrated sulphate)
	Carbonates: - Calcite ($CaCO_3$) - Aragonite ($CaCO_3$)

	Silicates: $(Mg, Fe)_2SiO_4$ - Olivine 1 (Fo_{64}) - Olivine 2 (Fo_{93})
B	**Phosphates:** - Apatite ($Ca_5(PO_4)_3(F, Cl, OH)$) **Silicates:** - Quartz (SiO_2) (sample of Rose Quartz)
C	**Sulphates:** - Polyhalite (hydrated sulphate), $K_2Ca_2Mg(SO_4)_4 \cdot 2(H_2O)$ - Epsomite (hydrous magnesium sulphate mineral) $MgSO_4 \cdot 7H_2O$ - Glauberite (sodium calcium sulphate) $Na_2Ca(SO_4)_2$

C	**Silicates:** • Phyllosilicates *Micas, the mica group of sheet silicate (phyllosilicate) ($X_2Y_{4-6}Z_8O_{20}(OH,F)_4$ in which *X* is K, Na, or Ca or less commonly Ba, Rb, or Cs; *Y* is Al, Mg, or Fe or less commonly Mn, Cr, Ti, Li, etc.; *Z* is mainly Si or Al, but also may include Fe^{3+} or Ti) - Phlogopite (magnesium mica), $KMg_3AlSi_3O_{10}(F,OH)_2$ - Biotite, phyllosilicate mineral within the mica group, $K(Mg,Fe)_3AlSi_3O_{10}(F,OH)_2$ *Chlorite, the chlorites are a group of phyllosilicate minerals, $(Mg, Fe)_3(Si, Al)_4O_{10}(OH)_2 \cdot (Mg, Fe)_3(OH)_6$ • Pyroxenes: $XY(Si, Al)_2O_6$, where X represents Ca, Na, Fe^{2+} and Mg and more rarely Zn, Mn and li and Y represents ions of smaller size, such as Cr, Al, Fe^{3+}, Mg, Mn, Ti, V and even Fe^{2+} - Augite $(Ca, Na)(Mg, Fe, Al, Ti)(Si, Al)_2O_6$ - Diopside $MgCaSi_2O_6$ - Wollastonite $CaSiO_3$ - Hypersthene $(Mg, Fe)SiO_3$ - Hedenbergite (iron pyroxene end-member), $CaFeSi_2O_6$, - Enstatite, (magnesium endmember of the pyroxene silicate mineral, $MgSiO_3$) - Bronzite(orthopyroxene) $(Mg, Fe)SiO_3$ • Amphiboles: $(A_{0-1}\,B_2\,C_5\,T_8\,O_{22}\,(OH, F, Cl)_2$ where ***A*** represents Na, K; *B* represents Na, Zn, Li, Ca, Mn, Fe^{2+}, Mg; ***C*** represents Mg, Fe^{2+}, Mn, Al, Fe^{3+}, Ti, Zn, Cr; and *T* represents Si, Al, Ti) - Hornblende, $Ca_2(Mg, Fe, Al)_5\,(Al, Si)_8O_{22}(OH)_2$ - Actinolite, amphibole silicate mineral, $Ca_2(Mg, Fe)_5Si_8O_{22}(OH)_2$ - Anthophyllite, an amphibole mineral, $(Mg, Fe)_7Si_8O_{22}(OH)_2$, magnesium iron inosilicate hydroxide • Olivine: Olivine 3, Olivine 4 ($(Mg, Fe)_2SiO_4$), Synthetic fayalite, Fe_2SiO_4

Table 6.1. List of samples that were a) identified by the RLS instrument, b) were more difficult to detect by the RLS instrument, c) that could not be identified by the RLS instrument. For ease of the reader all the well resolved spectra are repeated in the appendix at the end of this chapter.

In the following paragraphs we will discuss some of the parameters that led to Raman peaks in group *A* and *B* minerals being hard to detect and why minerals in group *C* could not be detected. Subsequently some recommendations will be given of how to improve the RLS

instrument for future space missions. Detections (or the lack of) are based on the following condition/parameters:

- The RLS instrument obtained Raman spectra only between ~ 200 and 3200 cm^{-1}.

This wavenumber range is limited by the specific design of the RLS instrument, notch filter and the use of Raman laser with a ~ 659 nm wavelength. The RLS instrument includes a notch filter that transmits the Raman emission, while filtering the laser excitation wavelength. This filter blocks Raman peaks with wavenumbers shorter than ~ 200 cm^{-1}.

Above 3200 cm^{-1}, the Raman emission is not detected on the RLS CCD detector. Based on the wavelength of the Raman laser excitation source (~ 659 nm), Raman emission is detected in the 3rd diffraction order. This order covers the wavelength range 650– 840 nm, i.e. Raman shift between ~ 200 and 3200 cm^{-1}. Because of the design of the grating, the 2nd diffraction order with the wavelength ranging only between 975 and 1256 nm reaches the CCD. So there is a gap between 840 and 975 nm on the CCD and Raman shifts higher than 3200 cm^{-1} cannot be analysed (see chapter two, section 2.4.3). As an example of this limited detection: O– H vibration modes in the spectrum of gypsum were not detected because they give Raman shifts in the 3300 to 3500 cm^{-1} region. A solution could be to change/rotate the position of the grating inside spectrometer to be able to detect the wavelength between 840 and 975 nm on the 3rd order or the 2nd order. Another solution is to change the laser wavelength so that the Raman shift above 3200 cm^{-1} have wavelength within the CCD range (see section 6.3.2).

- Grain size control

As discussed shortly in chapter 2 section 2.2.1, Raman emission can be created from the emissions by oscillating dipoles in molecules. These molecules are located within the small volume of the sample, which is illuminated by the Raman laser beam. The intensity of the Raman emission depends on the number of molecules in the volume illuminated by the Raman laser (see section 2.2.2). Therefore, the intensity of the Raman emission is dependnt on the number of the molecules involved in the emission. As a result, the reduction of the illuminated volume decreases the number of excited molecules and thus the intensity of the Raman peaks (e.g., Wang, et al., 1999). A fine-grained sample will generally have a lower volume to surface ratio than a larger crystal.

Previous researchers have shown that the most important factor that reduces the collecting efficiency of Raman emission is multiple reflections at various surfaces within and near the excitation volume (Wang, et al., 1999). As examples of the work presented here were RLS Raman spectra of gypsum and anglesite. These spectra contained strong background noise (see section 5.4). The effective power of the Raman laser beam was reduced by multiple reflections at the sample surfaces and at internal boundaries within the samples. In addition, due to all the reflections a proportion of the Raman emission photons would be outside of the collecting angle of the RLS instrument, (see part b in section 6.3). As a result the SNR is effectively reduced and this leads to problems in detecting weak Raman peaks.

The analyses performed on rose quartz provide an example of this sort of problem. Only one peak at 465 cm^{-1} was resolved in the Raman spectrum. This is the largest Raman peak resolved in quartz spectra but other peaks were completely obscured in the background noise, Fig 6.1. The Raman spectrum of quartz obtained by the Renishaw InVia Raman microscope is presented in Fig 6.2. Quartz was identified through a high peak near 464 cm^{-1} and weaker peaks at 263, 354, 393, 401, 508, 694, 806, 1080 and 1158 cm^{-1}. The reason for poor data from the rose quartz was twofold; the Raman laser could not be focused properly on the sample surface due to the amorphous nature of the sample and the extensive internal reflection of the laser light due to the fine grained nature of the sample. The advantage of the Renishaw InVia Raman microscope is that using the highest optical magnification (x 50) it was possible to adjust the focus of the laser to the desired spot on the sample surface and optimise the Raman signal. This example emphasises the need for a high quality optical system in any planetary RLS instrument with an automatic focus possibility to ensure that the optimal focal point can be achieved. The optical head on the RLS instrument was not versatile enough to allow fine tuning to achieve optimal Raman signals.

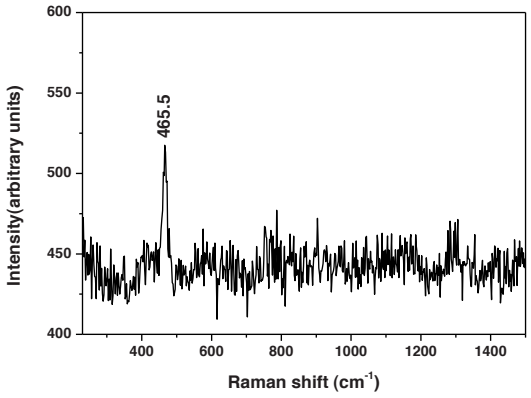

Figure 6.1. RLS Raman spectra of rose quartz.

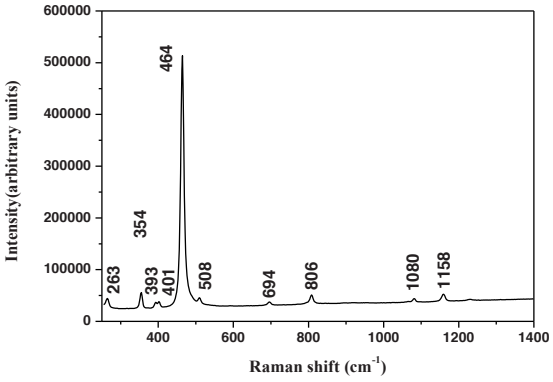

Figure 6.2. Renishaw Raman spectrum of rose quartz.

6.3 Suggestions for improving the RLS instrument

In this section, some suggestions for the improvement in the design of the RLS instrument are made. These suggestions are designed to provide feasible solutions to detect minerals that were hard to detect (or impossible to be detected) by the RLS instrument. These solutions are divided into two. First, solutions will be presented to increase the Raman peak intensity (increasing SNR). Second, suggestions are made to improve the spectral range of the RLS instrument above 3000 cm^{-1}. This suggestion will help to detect water vibration modes in hydrated minerals. We consider the detection of the water vibration modes in hydrated minerals vital for the study of the mineralogy of Mars to help understand the evolution of the planet.

6.3.1 Improving the Raman peak detection

An assessment of the Raman spectra obtained from minerals that were difficult to identify led to the following suggestions for the possible re-design or different measurement strategies to detect minerals:

a) Increase the laser power
b) Improvement of the Raman signal collection and transmission efficiency
c) Improvement of the SNR

6.3.1.1 Increase the laser power

One possibility to improve the Raman peak intensities is to increase the power of the Raman laser (chapter two, section 2.2.2). Based on the use of a second RLS instrument manufactured by TNO it was established that Raman intensity can be increased by use of a laser higher power that the 20 mW.

Increasing the Raman laser power, however, can cause destruction of some samples. The laser energy absorbed by the sample is correlated to different parameters such as the absorption coefficient of the sample and the mean irradiance at the laser focal point. The mean irradiance at the focal point of the laser depends on the laser power. If power increases, the irradiance at the focused point also increases (Delhaye et al., 1996). In a sample with a high absorption coefficient, laser light is absorbed. The absorption coefficient determines how far a particular wavelength can penetrate into a material light before it is absorbed. The greater power of the TNO laser caused damage to most hydrated and dark minerals. Therefore although increased laser power appears an attractive option there is limited benefit from increased power as minerals are damaged and it will no longer be possible to study hydrated minerals nor allow subsequent LIBS analysis. Therefore, when increasing the laser power, the properties of samples such as absorption coefficient and the wavelength of Raman laser should be reviewed. Based on the worked performed at the Vrije University Amsterdam

and TNO company we recommend an upper power limit of 200 mW but ideally any future planetary RLS instrument should have the potential to use variable power so that highly absorbent dark minerals and hydrated minerals can be analysed with lower laser power if needed.

6.3.1.2 Improvement of the Raman signal collection

- Decrease the RLS instrument spot size to analyse minerals with fine grain size

The RLS Raman laser has a spot size of 100 μm and it could not be focused on the fine grained mineral size samples such as the selected fayalite sample; ≤ 15 μm grain size. When analysing fine grained crystals, the main part of the Raman excitation light is diffracted in all directions or absorbed at the crystal grain interfaces, resulting in decrease of the Raman peak intensity. This was the reason that the detection of fayalite was impossible with the RLS instrument and the peaks obtained on rose quartz were poorly resolved. On Mars the ExoMars mission can expect to encounter numerous fine grained minerals in environments that will be selected for detailed analysis; areas of past active water-rock interaction and sulphate formation. Reduction of the laser spot size is therefore recommended. The down side of such an approach is that far more analyses will be needed to characterize the mineralogical variation in individual rocks. Reduction of the spot size from 100 to 10 μm for example will result in the analysis of a factor of 100 less material. Although this approach will lead to better resolution of individual minerals the decreasing the spot size will result in the increase in the amount of energy per volume and potentially destroy the sample. Therefore, the recommendation for variable power output is again emphasised. An ideal compromise would be to have variable magnification options on the optical head of the RLS instrument. Without such flexibility many minerals will not be identified (large spot size) or potentially destroyed (high laser power and small spot size). More detailed research needs to be conducted on rocks considered representative of Martian surface environments to have a better understanding of the potential trade-offs required between laser spot size and power. Such work particularly needs to take into account that most Martian surfaces are not flat, even at the 100 μm scale. Methodologies are needed to optimise analyses of true samples as opposed to the laboratory samples measured in this study. Time constraints related to the manufacture of the MASC prevented this PhD research from conducting such work, which was part of the original research plan. We are totally aware that the recommendations made above for variable laser power and magnification will have major repercussions for the overall power usages, mass and size of any future instrumentation. However, the practical experience of using the RLS instrument make it clear that performance is far below that of a research instrument and any Flight Model needs greater flexibility than the current EB instrument.

- Improvement in the RLS instrument design

TNO, the designers and manufacturers of the RLS instrument, undertook a detailed analysis of the optical efficiency of the RLS instrument. A power meter was used:

- To measure the amount of Raman laser light energy from Raman laser excitation source to the sample surface, Table 6.2.
- To measure Raman emission energy from the sample surface to the spectrometer and CCD, Fig 6.3.

Light loss in the instrument is expected to be caused by absorption of the different optical components (such as fibres, mirrors and filters), optical misalignment and inefficient coupling between components. The contribution of different components in the loss of Raman laser excitation light (before reaching the sample) is presented in table 6.2. At the laser output, 6.62 x 10^{16} photons per second are emitted but at the sample surface only 1.6 x 10^{16} photons per second are measured. These data emphasise that optimal alignment of the fibres and connectors is essential to avoid the loss of the Raman laser excitation light in the RLS instrument design.

Source	laser	6.62 x 10^{16} photons/s
Optical interface	Fibre FC optical fibre connectors (use in high-vibration environments) Fibre coupling connector	85% 90% 80% 55%
	Overall transmission	24.25%

Table 6.2. Percentage of Raman laser light transmitted by the different optical components from the Raman laser excitation source to the sample surface.

In addition, Raman emission was also lost in different parts of the RLS instrument from the sample surface to the spectrometer. First, Raman emission is emitted in all directions from the sample surface and the RLS instrument collects the Raman emission within a cone with a half angle of 12.7 degrees. Therefore, the Raman emission, which was emitted in different directions outside this cone, was lost: only ~ 1% of the light is indeed collected (half angle of 12.7 degrees corresponds to a solid angle of 0.15 steradian, which is 1% of the solid angle of a full sphere). Additional Raman emission was lost inside the optical head, at optical interfaces and finally inside the spectrometer. Therefore, only approximately one Raman photon in 10000 produced at the sample was detected by the CCD. A graph summarising the loss of Raman emission from the sample surface to the CCD is shown in Table 6.3. This graph demonstrates that Raman emission was mostly lost at the collection angle. Then there are successive losses at optical interfaces. Almost half of the Raman emission was lost significantly in the spectrometer. Consequently, re-design of the collection angle and spectrometer can be a potential option to avoid the Raman emission loss.

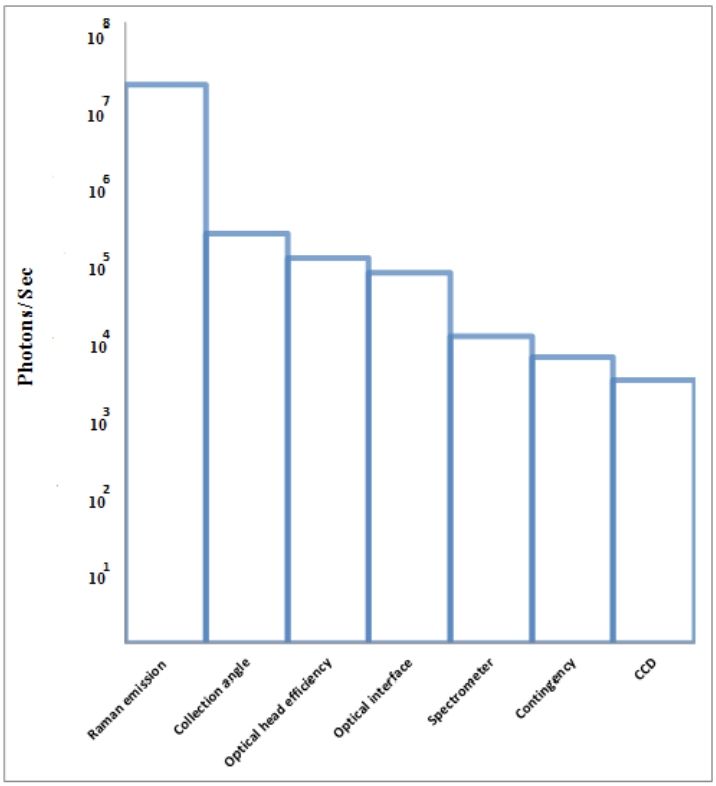

Table 6.3. Graphs of Raman emission loss from the sample surface to the CCD. Note the graph has a logarithmic scale (TNO document-ESA-RLS-RP-2008).

6.3.1.3 Improvement in the SNR

Given the relatively inefficient production of Raman signals in the RLS instrument compared to laboratory instrument (such as the Renishaw InVia Raman microscope that we used for comparison studies), improvement in SNR of the RLS instrument is potentially of great benefit. Noise sources can be classified into two types: temporal and spatial. Examples of temporal noise were shortly discussed in section 2.4.3.1 and are:

- Shot noise,
- Output amplifier noise,
- Dark noise,

Spatial noise sources contain dark current non-uniformity and photo response non-uniformity. Some spatial noise can be removed for example by applying frame subtraction or gain/offset correction techniques to the data obtained from the CCD.

Temporal noise varies with time and can be decreased by increasing the integration time. Integrating for longer time on the CCD or stacking the Raman spectra will improve the SNR. These two solutions will be treated in the following sections to find the more relevant technique to improve the SNR in the RLS instrument.

- Increase the acquisition time to decrease shot noise

To assess the best way to improve the SNR a series of simple experiments were performed with different acquisition times where a straightforward spectrum such as calcite was examined. Raman spectra of calcite were obtained with the acquisition time of 9, 30, 40, 90 and 100 s. The SNR of the weak peak at ~ 1087 cm^{-1} at the same spot of a calcite sample was 70.3, 80, 180, 196.4 and 140 counts for acquisition times of 9, 30, 40, 90 and 100 s respectively, Table (6.4). Unfortunately, SNR of the peak at the acquisition time of 100 decreases, because the lower laser was unstable and produced multiple wavelengths (Fig. 6.3). Further experimentation established that the laser wavelength is definitely unstable with an acquisition time longer than 40 s irrespective of the numerous remedial measures applied. Therefore, in this PhD research an acquisition time of 40 s was selected to avoid the instability of the laser excitation light and for the detection of weak peaks for all measurements. Clearly it is unviable to manufacture the RLS instrument that contains an unstable laser and this point is not discussed in any further detail in this work.

The integration time required to obtain a useful spectrum also depends on the selected samples. Raman spectra of group B and C (Table 6.1) were obtained with longer integration times, but even for long acquisition time such as 100, 120 s and 160 s Raman peaks for minerals in group *C* were not detected.

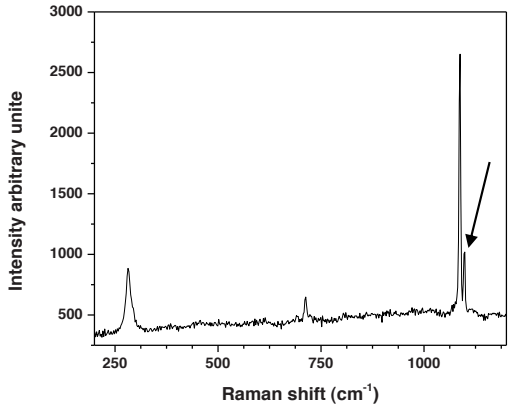

Figure 6.3. RLS Raman spectrum of calcite with acquisition time of 100 seconds. Laser excitation wavelength was unstable at 100 s acquisition time leading to a "ghost peak" at 1087 cm^{-1}; marked with the arrow.

Acquisition time	Noise	S	S/N
9	8	562.5	70.3
30	9	720	80
40	12	2160	180
90	14	2750	196.4
100	15	2100	140

Table (6.4). The SNR of the weak calcite peak at ~1087 cm^{-1} for acquisition times of 9, 30, 40, 90 and 100 s.

- Improvement in the SNR by stacking Raman spectra

Stacking a series plots is expected to show benefit as some of the random noise will be cancelled out thereby producing better SNR. The stack Raman spectrum is presented in Fig 6.4. Eight Raman spectra of a calcite sample were collected to determine if the SNR increases. However, as already mentioned, the laser excitation source was unstable and "ghost peaks" were present in the calcite Raman peaks spectrum. Therefore, experiments performed with the RLS instrument at the VU did not find this method useful. However, in using the Renishaw InVia Raman microscope, we successfully adopted this approach and it is therefore recommended that the operational software of the RLS has the flexibility to vary both integration time and stack spectra.

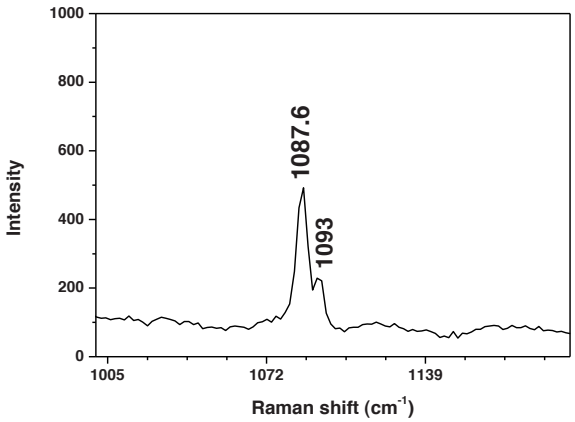

Figure 6.4. Stack plots of eight Raman spectra of a calcite sample (with 40 s acquisition time) from 1000 to 1200 cm^{-1}. The integrated spectrum shows that the laser excitation wavelength was unstable as there were two ν_1 intense peaks results from the symmetric stretching of CO_3 group at 1087.6 and 1093 cm^{-1}.

In the next generation of the RLS instrument, we do not expect problems with laser stability. Therefore, we recommend that the software that controls integration times of the CCD can be varied dependent upon an initial analysis. RLS instrument operates on Mars, it needs to have a very flexible analytical protocol. For instance, measuring carbonate is relatively easy and

the problem will be that large peaks may over saturate the CCD. Long integration times for all analyses are therefore not possible. A complementary solution would be to stack multiple integrations. But this will require additional processing power and could be limited by processing power within the Rover. As well, according to section 2.4.3 the combination of the multiple integration times may instead increase read-out noise. Increasing the acquisition time is then a better solution. So we recommend to first increase the acquisition time as much as possible, then to stack different spectra if still necessary.

6.3.1.4 Decrease thermal noise in the CCD cooling system

As discussed at section 2.4.3.1 electrons not related to the absorption of photons are generated within the CCD by physical processes within the CCD itself. The number of these electrons generated mainly depends on the operating temperature of the CCD. Based on the Raman spectra of some potentially key minerals in respect of Mars exploration that were studied in this thesis (e.a., gypsum, barite and anglesite at low temperature), it was not always possible to detect all their weak peaks, even when the CCD was at its lowest temperature (~ -40 °C). Given the expected sampling methodology of ExoMars, analyses of multiple minerals will be a common event and so it will be vital to detect as many Raman peaks as possible so as to be able to recognise all the minerals that contribute to a single Raman spectra; the more Raman peaks recognised the easier it will be to recognise multiple minerals. Our experimentation established that reduced dark noise from the CCD when operated at ~ -40 °C, makes peak detection limit about two times better than at -30 °C. Clearly further improvement in peak detection will provide benefits in the identification of weak Raman peaks. Two recommendations are therefore made. First, to replace the current CCD with the better and more modern CCD that is more sensitive and has lower dark noise. Such instrumentation is already available (Holland et al., 2004). Second, re-design of the CCD cooling circuit is required to reduce the operating temperature of the CCD to below -40 °C. The latter recommendations has a potentially significant implication for the power usageof the ExoMars rover, however, given the generally low temperatures encountered on the Martian surface, especially at night, it should be possible to accommodate a more efficient CCD cooling system with low weight and power consumption.

6.3.2 Improve the spectral range of RLS instrument above 3000 cm^{-1}

A major conclusion of this thesis is that the spectral range of the RLS spectrometer is too limited; as explained in section 6.2. Most crucial is the lack of capability to detect peaks associated with water vibration modes in minerals above 3000 cm^{-1}. This is a fundamental design limitation of the RLS instrument and is a reason why the Raman only instrument now being prepared for ExoMars will have a different spectrometer design and a larger spectral range.

In principle it is possible to re-align the optics of the RLS spectrometer to allow the detection of O– H Raman vibration modes in the 3300 to 3500 cm^{-1} region. However, as the RLS

instrument is the property of ESA and it was not possible to make major modifications to the spectrometer; e.g., re-alignment of the grating. Our research has established that it is possible to detect Raman peaks > 3000 cm^{-1} when the position of the grating or the wavelength of the excitation laser light is changed. Work led by Dr A. Collin resulted in the introduction of a new laser system and replacement of the laser optical system. Several laser excitation sources were reviewed to select a suitable wavelength for detection of the O– H vibration mode of water. Figure 6.5 shows the Raman spectra of an amphibole sample with different laser excitation sources. The O– H vibration mode of water is identified with 473 and 532 nm Raman lasers. According to the data shown in chapter two (section 2.4.3) Raman laser with a 532 nm wavelength did not completely fit in the RLS CCD range. Based on the wavelength of the Raman laser excitation source (532 nm) Raman emission is detected in the 4^{rd} diffraction order that covers the wavelength range 504– 630 nm, i.e. Raman shift until 2900 cm^{-1}. Because of the design of the grating, the 3^{rd} diffraction order with the wavelength ranging between 650 and 840 nm reaches the CCD. So there is a gap between 650 and 630 nm on the CCD and Raman shift between 2900 and 3400 cm^{-1} cannot be analysed (see chapter two, section 2.4.3). In contrast the range of the Raman spectrum obtained by a 473 nm wavelength laser, was found to fit in the fourth and fifth diffraction orders in the CCD detector (200 to ~ 5300 cm^{-1}). In addition, this laser is small (~ 10 cm x 6 cm) and commercial Raman filters were available. Therefore, this commercial laser with band filter and ultrasteep edge filter was selected for identification of the O– H vibration mode of water with the RLS instrument.

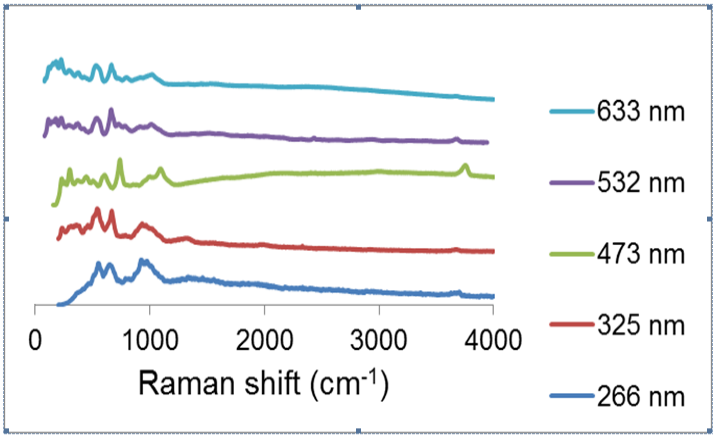

Figure 6.5. Influence of the laser wavelength on the water signal in amphibole, taken from the commercial Raman instrument in Lille, France. The Y axis is arbitrary units and all spectra are normalised to their highest peak and vertically offset for legibility. Water peak is observed with laser with 473 nm wavelength.

By installing the ~ 473 nm laser on the RLS instrument, detection of O– H vibration modes of gypsum were possible as shown in Fig 6.6. In the gypsum Raman spectrum, the peak around 3300 and 3500 cm^{-1} are generated by symmetric stretching (ν_1) and antisymmetric (ν_3) stretching vibration modes of water respectively. ν_2 bending vibration mode of water as a

weak mode (at ~ 1880 cm^{-1}) was not detected. This approach emphasises that a redesign of the RLS instrument would allow better identification of minerals by Raman spectroscopy while maintaining a comprehensive coverage of the LIBS spectrum.

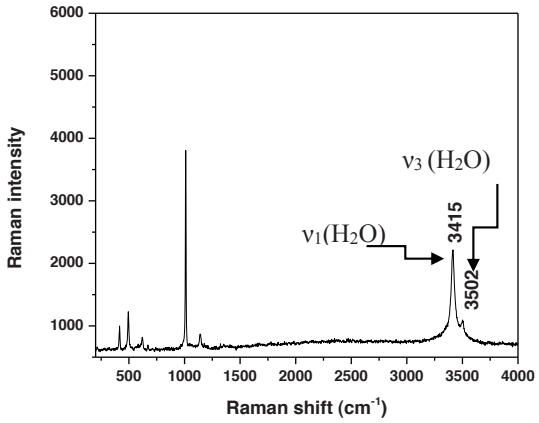

Figure 6.6. RLS Raman spectrum of gypsum, with 473 nm excitation laser.

6.4 Conclusion

The fundamental conclusion is that the RLS instrument was able to analyze a group of selected minerals under Martian conditions inside the MASC validating the basic principle that a combined Raman/LIBS instrument is applicable for planetary missions. A second major conclusion is that no significant variations in Raman spectra were determined due to changes in environmental conditions pertinent to Mars. Importantly it has been shown that it is possible to use changes in Raman spectra to determine the composition of olivine with the RLS instrument by monitoring variations of a doublet peak in the 700– 900 cm^{-1} range. Moreover, recognition of carbonates and different sulphate minerals was also possible. RLS Raman spectra for barite, anglesite and gypsum have clear differences that can be related to the different mineral structures. In all spectra, there were variations in peak positions and splitting, due to the influences of the different metal cations. In the case of barite and anglesite, the wavenumber of the vibrational modes of SO_4 tetrahedra, decreases with an increase of the atomic mass of the metal cations. In addition, Raman peaks shift to higher wavenumbers with an increase of the stretching force constant of S– O bonds.

The use of the RLS instrument inside the MASC chamber has raised a series of practical aspects of Raman analysis that need to be addressed before a RLS instrument is sent on a planetary mission. These mostly concern the analysis of typical surfaces on Mars. The RLS instrument was unable to detect Raman signals from several mineral samples that were

identified by the commercial Renishaw InVia Raman microscope, even though all the samples were prepared as flat surfaces. The fact that fine grained samples (< 15 μm) were difficult to analyse emphasises that on the non flat surfaces that will be encountered on Mars it will be even more difficult to obtain high quality Raman spectra. We recommend extensive further testing of the RLS EB instrument and the newly designed Raman-only instrument for ExoMars on samples that will be more typical of Martian surfaces. The work carried out to date, although under Martian conditions, was essentially under laboratory conditions. More rigorous assessments of the effects of variable grain size and surface morphology are needed, as the intensity of the Raman peak is determined not only by instrument optics, but by the sample properties. The influence of the crystals properties (such as grain size, surface relief, colour and absorption coefficient) on the peaks intensity needs to be studied.

We identified several aspects of the RLS instrument that were sub-optimal and a series of recommendations were made of how to improve instrument performance. These are summarised below.

Recommendation	**Goal**
- Select a suitable stable Raman laser source	- Accurate and reproducible Raman spectra
- Increase the laser power	- Improving the detection limits of minerals
- Decrease the RLS instrument spot size	- Ability to identify minerals of small grain size
Improving the RLS optical design - Re-design spectrometer - Shorter optical fibres - Use less connectors	- To increase SNR and optical transmission
- Improve the CCD cooling system	- Increasing SNR (decrease thermal noise)
- Change the angle of the grating or apply a shorter wavelength laser source	- To expand the Raman spectral range to above 3000 cm^{-1} to include water

Table 6.5. Recommendations for improving the RLS instrument.

The current RLS instrument has been shown to be viable as a Raman instrument and initial work with LIBS has also produced valuable data (Colin et al., 2012). Coupled with the proposed improvements above we are confident that the use of a combined Raman-LIB spectrometer will be a valuable addition to the contact instrument package of future planetary missions.

6.5 References

Delhaye, M. et al., (1996), Chap 3: Instrumentation. in: Turrell G and Corset J (eds) Raman Microscopy. Developments and Applications. Academic Press, London.

Colin, A. et al., (2012), Sensitivity study of lunar soil water content measurements using a combined Raman/LIBS instrument. ESA/ESTEC conference: Scientific Preparations for Lunar Exploration, ESA/ESTEC- Noordwijk (The Netherlands) – poster.

Holland A. D. et al., (2004), CCDs for the rotational velocity spectrometer on GAIA doi:10.1117/12.517151.

Wang, A., (1644), Some Grain Size Effects on Raman Scattering Intensity for In Situ Measurements on Rocks and Soils Experimental Tests and Modeling, Lunar and Planetary Science XXX, 1644.

Appendix

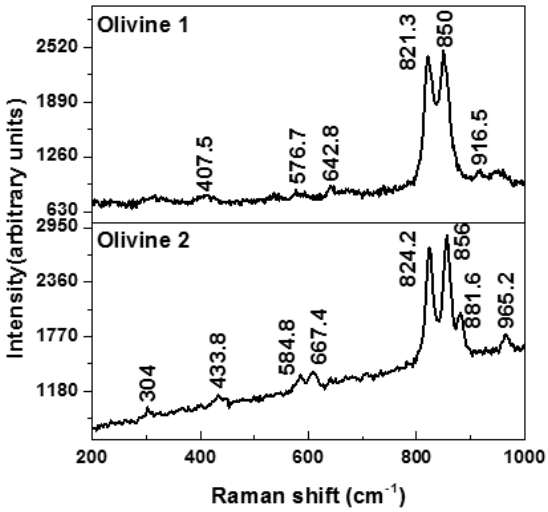

Figure 1. The Raman spectra of olivine 1 (Fo_{64}) and olivine 2 (Fo_{93}) taken with the Renishaw InVia Reflex confocal Raman microscope for the 200-1000 cm^{-1} region.

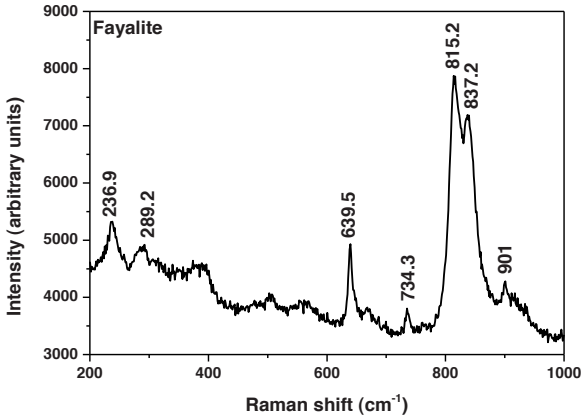

Figure 2. The Raman spectra of fayalite (Fo_{01}) taken with the Renishaw InVia Reflex confocal Raman microscope for the 200-1000 cm^{-1} region.

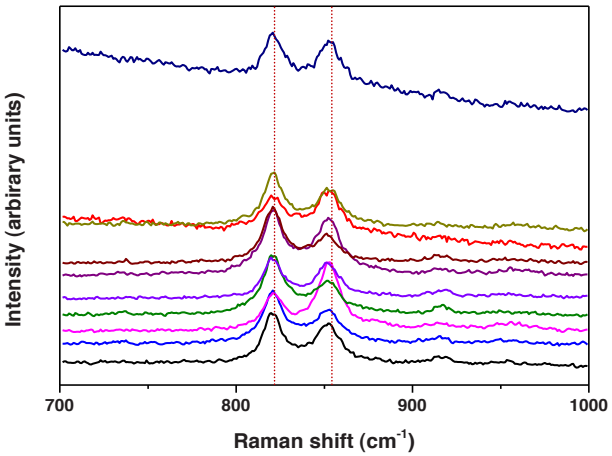

Figure 3. The Raman spectra obtained from 10 random grains of olivine 3 taken with the Renishaw InVia Reflex confocal Raman microscope for the 700-1000 cm^{-1} region. Spectra are vertically offset for legibility.

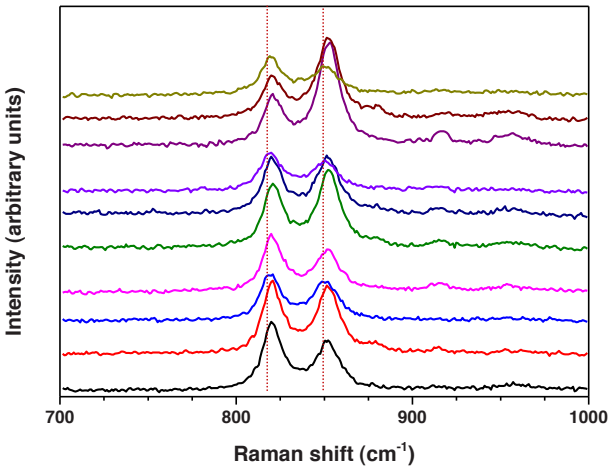

Figure 4. The Raman spectra obtained from 10 random grains of the olivine 4 taken with the Renishaw InVia Reflex confocal Raman microscope for the 700-1000 cm^{-1} region. Spectra are vertically offset for legibility.

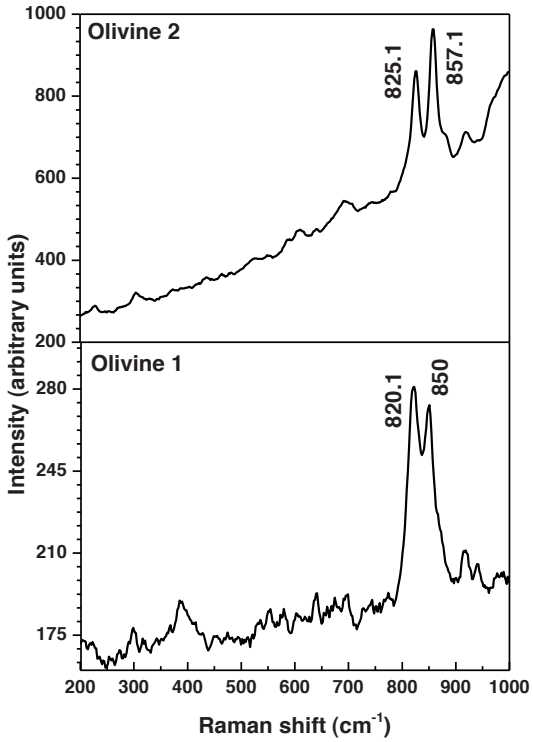

Figure 5. The RLS Raman spectra of olivine 1 and olivine 2 obtain under vacuum condition at 10 °C.

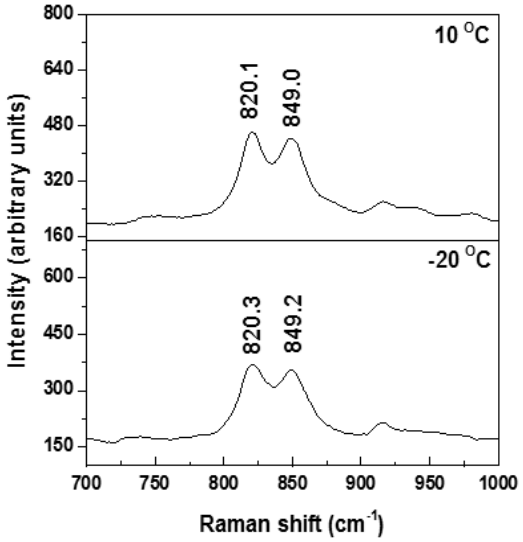

Figure 6. RLS Raman spectra of olivine 1 in the range 700– 1000 cm^{-1}, the measurement conditions are under vacuum condition at +10 and -20 °C.

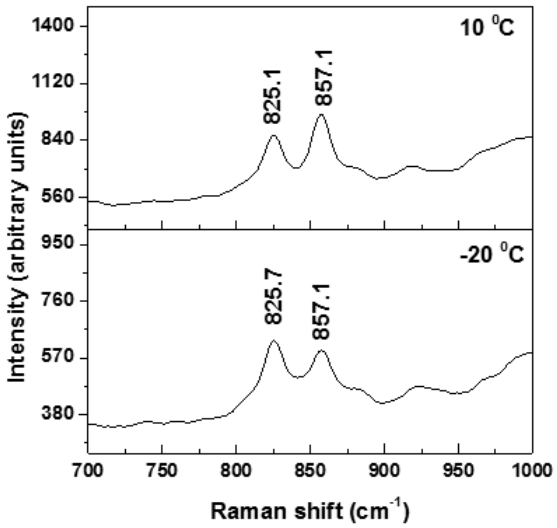

Figure 7. RLS Raman spectra of olivine 2 in the range 700– 1000 cm^{-1}, the measurement conditions are under vacuum condition at +10 and -20 °C.

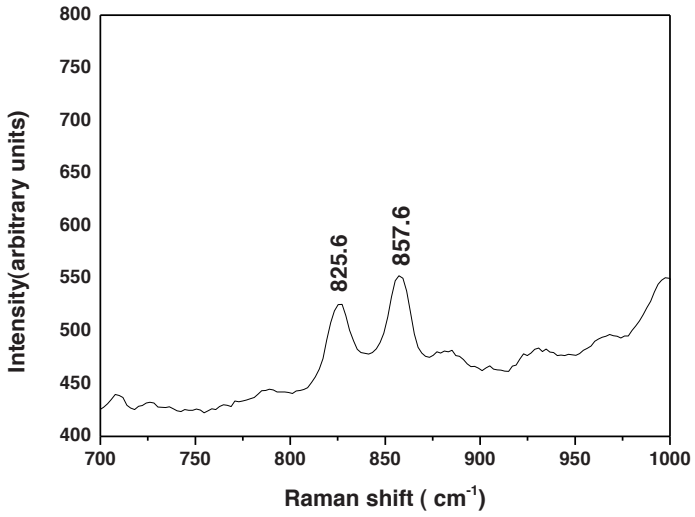

Figure 8. RLS Raman spectra of olivine 2 in the range 700– 1000 cm^{-1}, the measurement condition is CO_2 atmosphere with -20 °C.

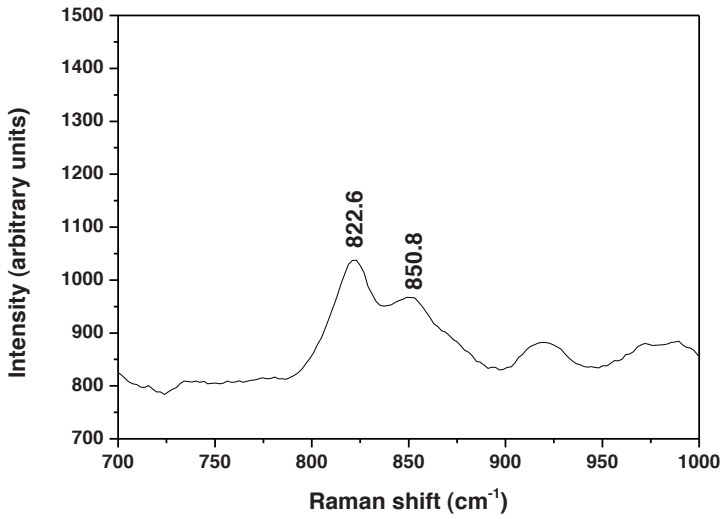

Figure 9. RLS Raman spectra of olivine 1 in the range 700– 1000 cm^{-1}, the measurement condition is CO_2 atmosphere with -20 °C.

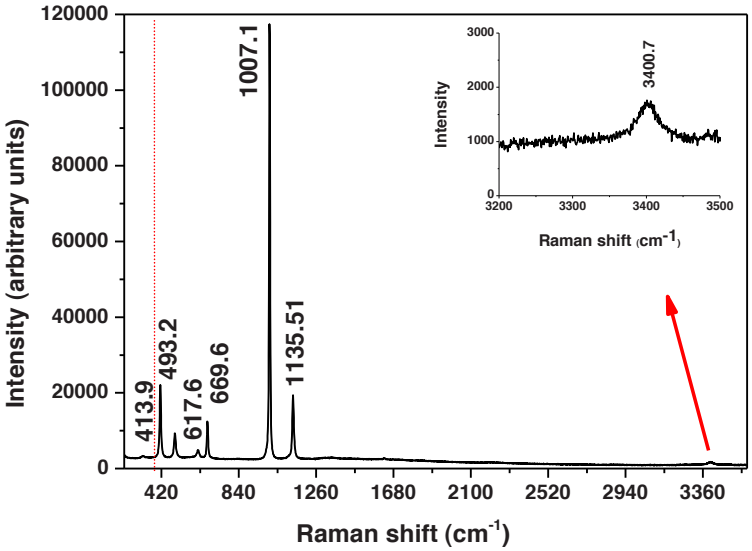

Figure 10. Gypsum Raman spectrum taken with the Renishaw InVia Reflex confocal Raman microscope. The peak at 3400.7 cm^{-1} is attributed to O─ H vibration mode of water in the gypsum structure. The Raman spectrum of gypsum is separated into two parts, external vibrations (< 400 cm^{-1}) and internal vibrations (400─ 1200 cm^{-1}) of the sulphate groups.

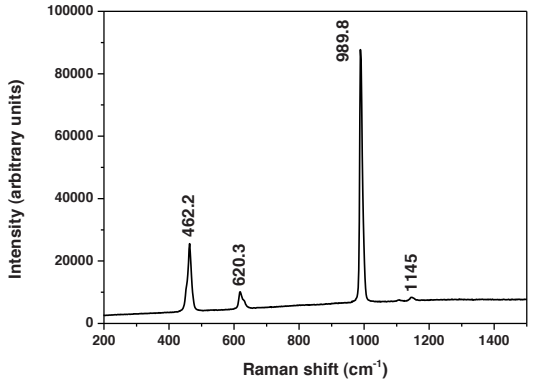

Figure 11. Barite Raman spectrum taken with the Renishaw InVia Reflex confocal Raman microscope.

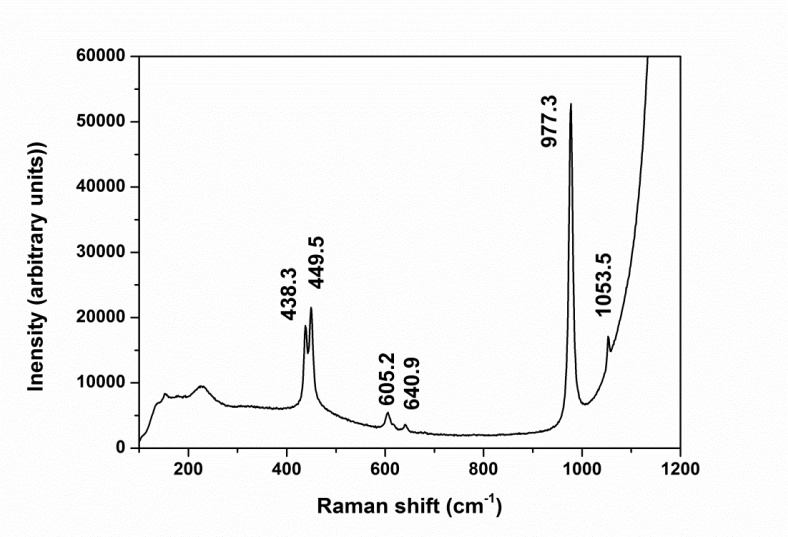

Figure 12. Anglesite Raman spectrum taken with the Renishaw InVia Reflex confocal Raman microscope.

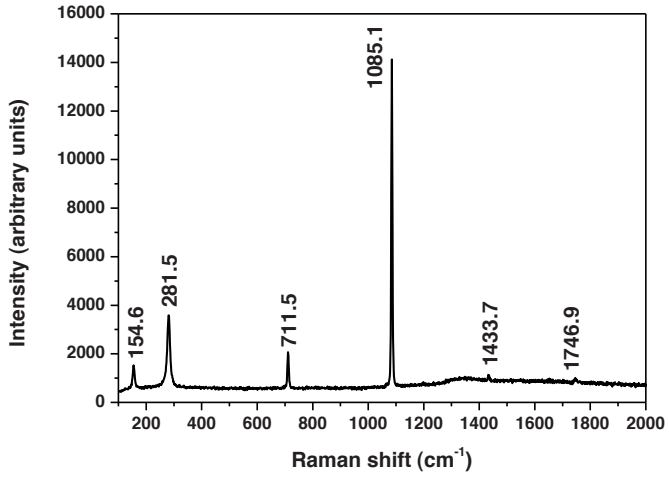

Figure 13. Calcite Raman spectrum taken with the Renishaw InVia Reflex confocal Raman microscope.

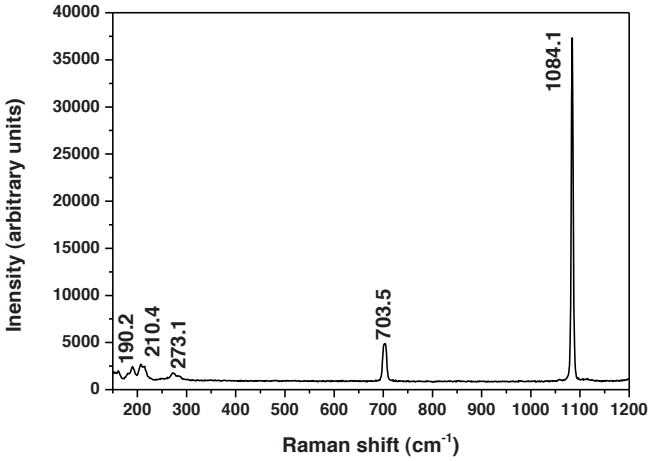

Figure 14. Aragonite Raman spectrum taken with the Renishaw InVia Reflex confocal Raman microscope.

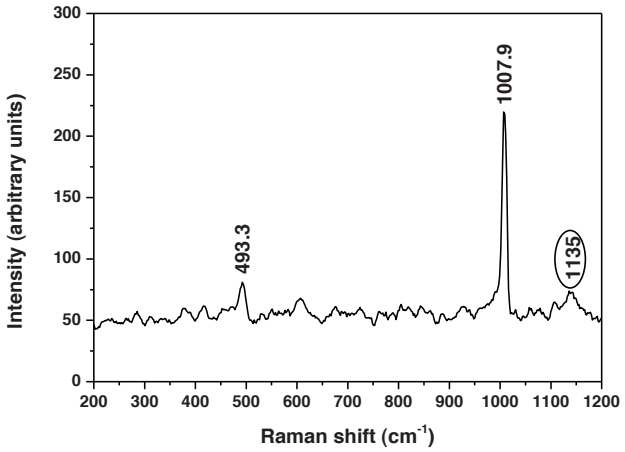

Figure 15. Gypsum RLS Raman spectrum under vacuum at 10 °C. The peak at ~ 1135 cm^{-1} is poorly resolved from the background noise.

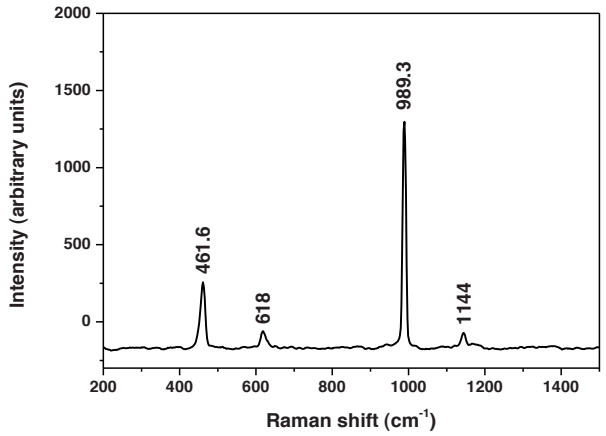

Figure 16. RLS Barite Raman spectrum under vacuum at 10 °C.

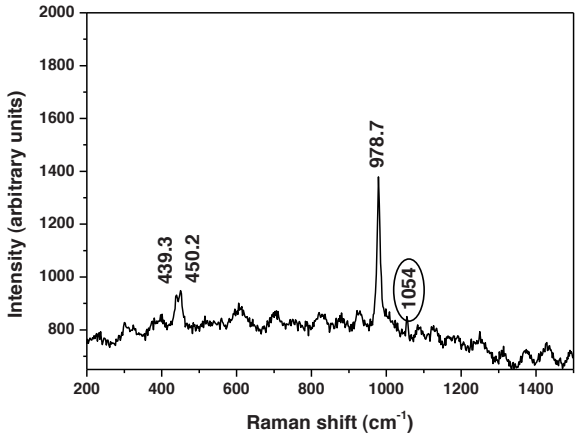

Figure 17. RLS anglesite Raman spectrum under vacuum at 10 °C. The possible peak at 1054 cm^{-1} was poorly resolved from the background at 10 °C.

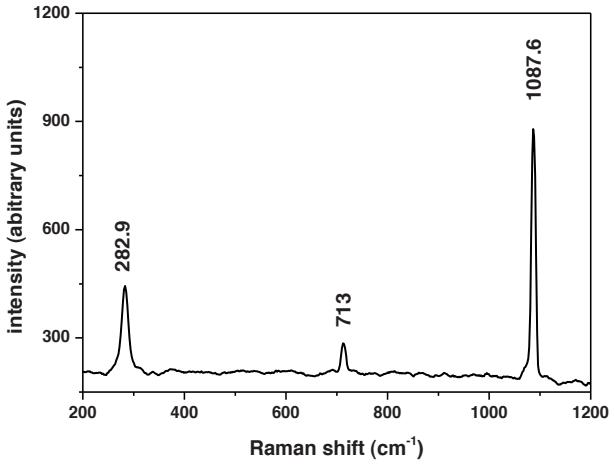

Figure 18. RLS calcite spectrum under vacuum at 10 °C.

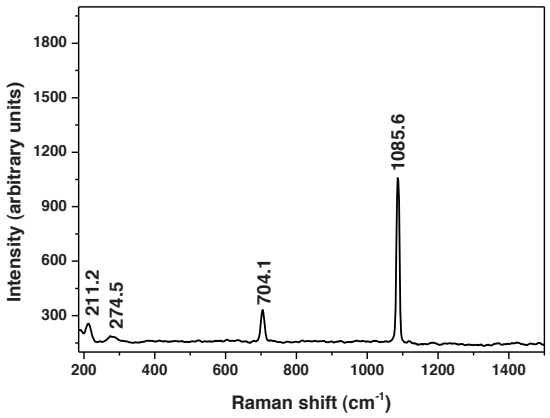

Figure 19. RLS aragonite Raman spectrum under vacuum at 10 °C.

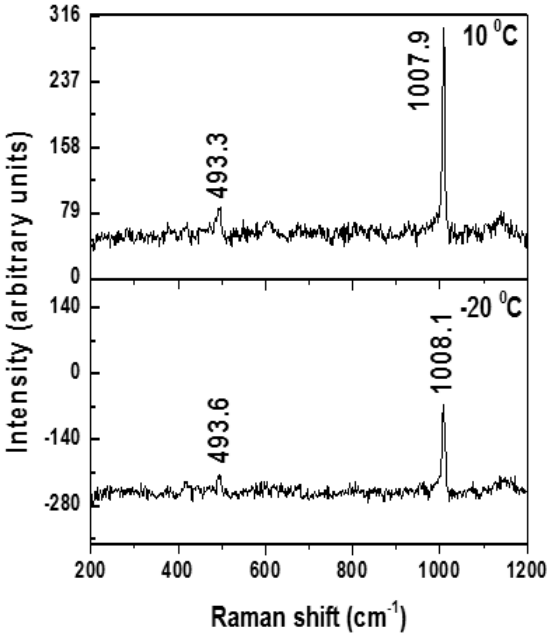

Figure 20. Raman spectra of gypsum in the range 200– 1000 cm^{-1}, the measurement conditions are vacuum at +10 and -20 °C.

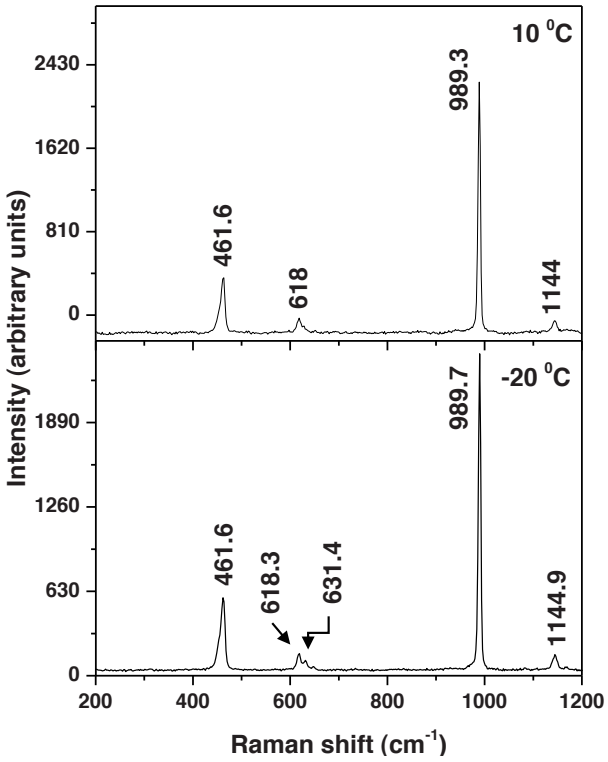

Figure 21. Raman spectra of barite in the range 200– 1000 cm^{-1}, the measurement conditions are vacuum at +10 and -20 °C.

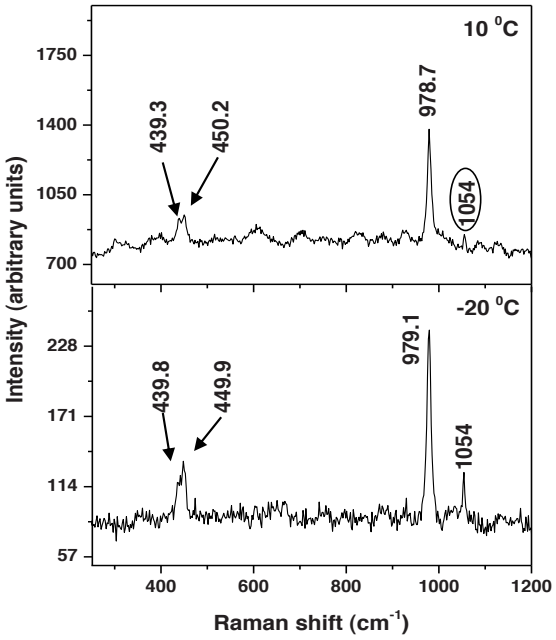

Figure 22. Raman spectra of anglesite in the range 200– 12000 cm^{-1}, the measurement conditions are vacuum at +10 and -20 °C. The possible peak at 1054 cm^{-1} was poorly resolved from the background at 10 °C.

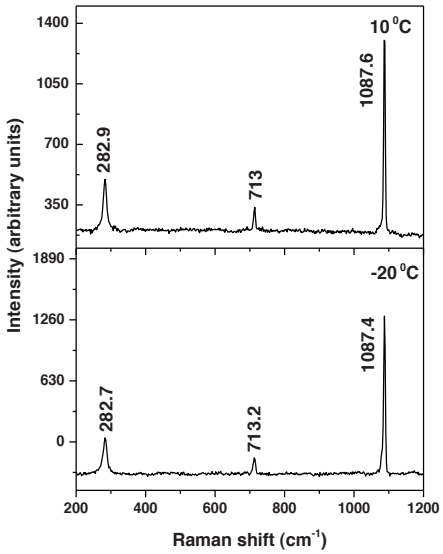

Figure 23. Raman spectra of calcite in the range 200– 12000 cm^{-1}, the measurement conditions are vacuum at +10 and -20 °C.

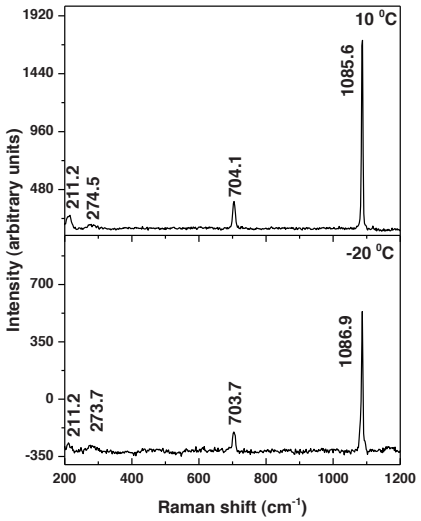

Figure 24. Raman spectra of aragonite in the range 200– 12000 cm^{-1}, the measurement conditions are vacuum at +10 and -20 °C.

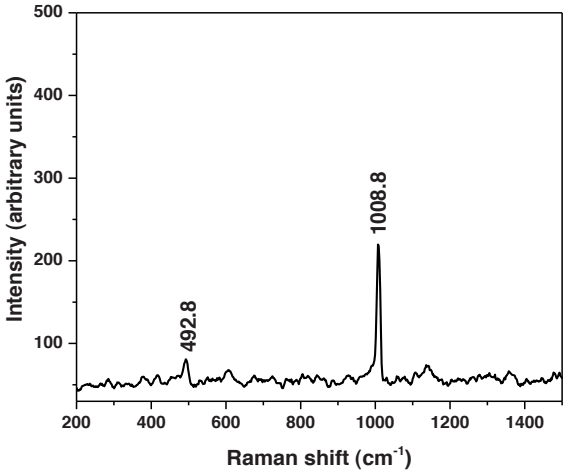

Figure 25. RLS gypsum Raman spectrum under 8 mbar CO_2 atmosphere at -20 °C.

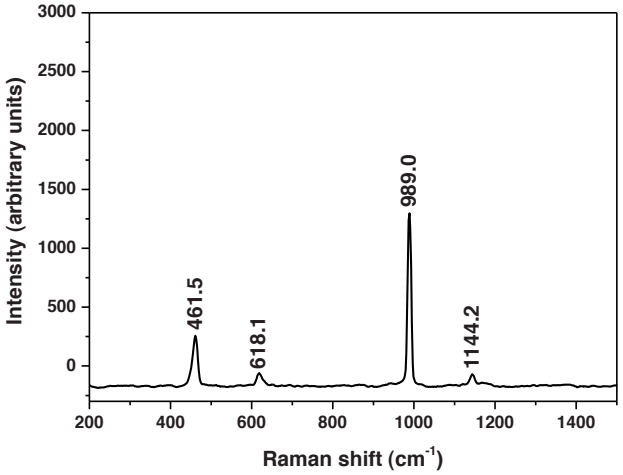

Figure 26. RLS barite Raman spectrum under 8 mbar CO_2 atmosphere at -20 °C.

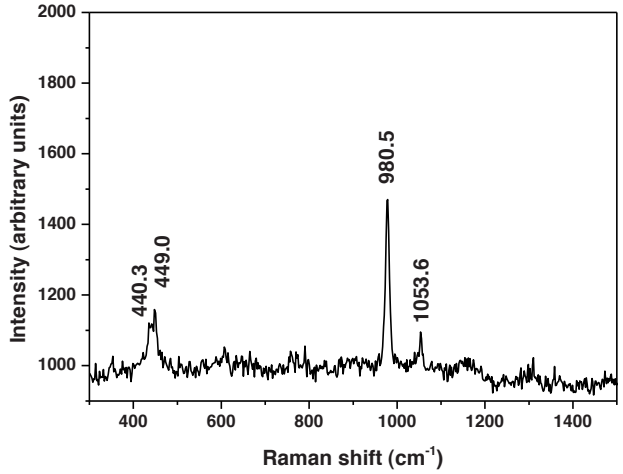

Figure 27. RLS anglesite Raman spectrum under 8 mbar CO_2 atmosphere at -20 °C.

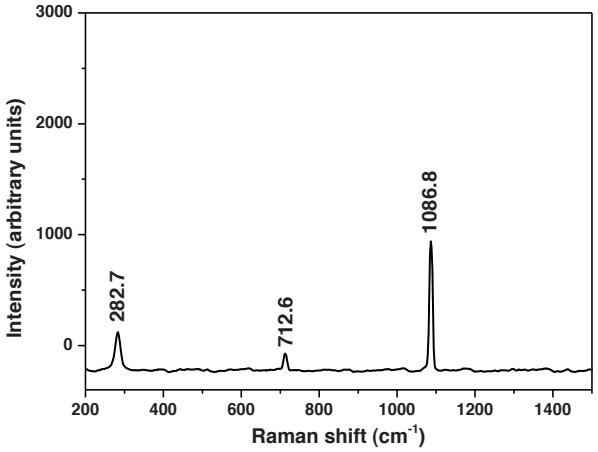

Figure 28. RLS calcite Raman spectrum at -20 °C under 8 mbar CO_2 atmosphere.

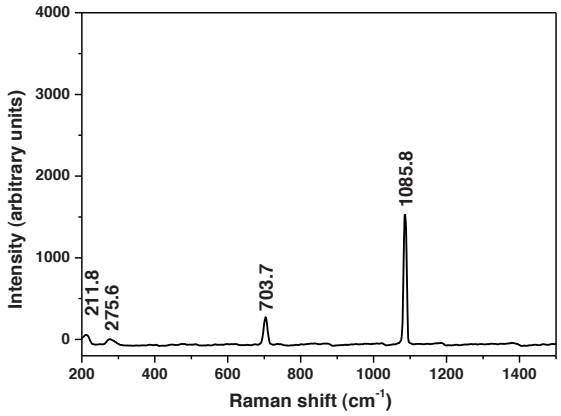

Figure 29. RLS aragonite Raman spectrum at -20 °C under 8 mbar CO_2 atmosphere.

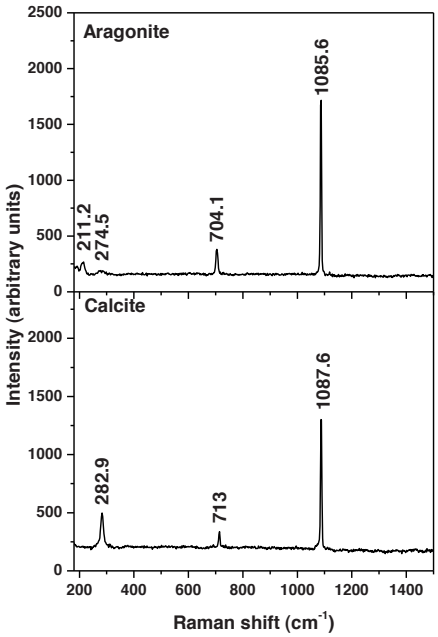

Figure 30. RLS Raman spectra of aragonite and calcite under vacuum at 10 °C in order to classify their mineral structure.

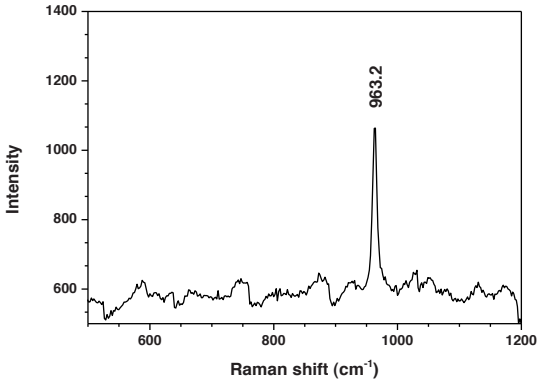

Figure 31. RLS Raman spectra of apatite

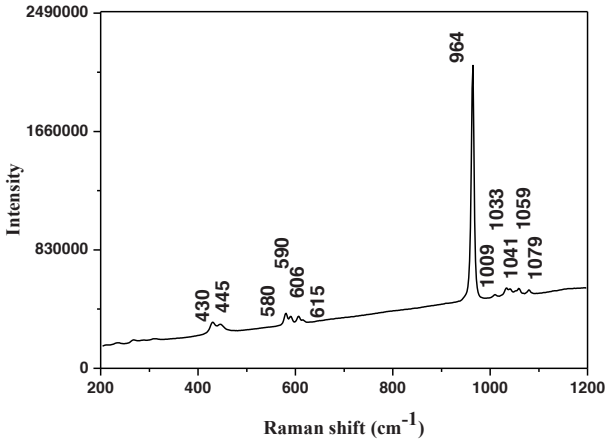

Figure 32. Renishaw Raman spectrum of apatite.

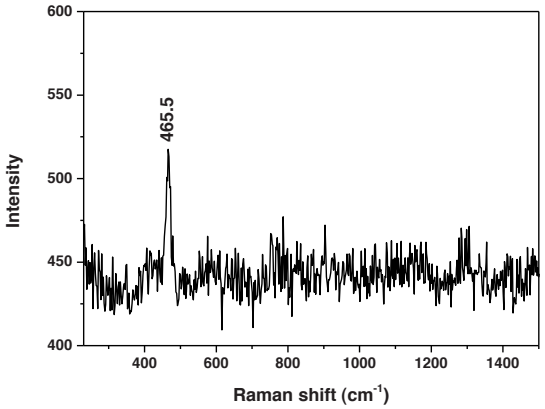

Figure 33. RLS Raman spectra of rose quarts.

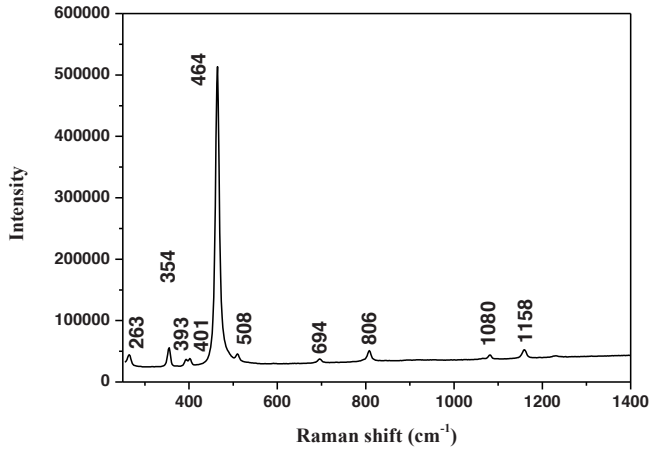

Figure 34. Renishaw Raman spectrum of rose quartz.

Acknowledgements:

Professor Davies has been the main supervisor of this PhD research. I would like to thank him first of all. The time he spent on this research is appreciated. He introduced me to the people from the ExoMars programme, who proved to be very important and so helpful; thanks to Berit, Erik, Ian and Richard because I learned different aspects of my research from them. Maria deserves a special message as she was readily available. I appreciated our collaboration and that she were available even over the phone.

I had the privilege to work in a pleasant environment in the Petrology-Deep Earth and Planetary Science department. For this I would like to thank my colleagues; Elodie, Daphne Jelle, Laura, Mirjam, Nachiketa, Sonja, Jane, Janne, Jeilie, Jessica and Josepha. Furthermore, I would like to thank Wim, Fraukje, Wynanda, Bas, Peiter, Frank, Richard and Roel for their support and great friendship during my stay in the department.

Extra special and heart-felt thanks go out to:

- Esther, we shared our office and accompanied each other on a daily basis. She was not only my office mate but also a good friend.

- Aurelia, she was a great help in my research as she made a major contribution in the calibration of the CCD and also developed several matlab programs. For these and many other reasons I appreciate her time and support.

- The Vrije University technical staff, most notably Onno, Ron, Daniel, Rob, Nick and other colleagues. With their input and guidance in this entire project I could make it to the finish line.

- Fenny, she gave me such useful support and guidance both for my career and private life.

- Jan-Hein, Freek and other colleagues and technicians at the Laser Centre at the Vrije University, with whom I shared the challenges of an unstable laser and many other technical challenges.

- My friends Irene, Stephan and Javier; they were some of the people that pulled me through in rough times.

- The ones standing closest to me are my family such as my sister Razi, my brothers Reza and Roozbeh. They provide their moral support and encouragement. My mother has been a particularly inspiring role model who always stimulated me to continue my study in times that I was struggling. An extra special mention to Emile Gerard for being the one that always stood right next to me in the final years of my research.

Finally I would like to dedicate this thesis to my father, who unfortunately can no longer be with us.

Curriculum vitae

Raheleh motamedi was born in Esfahan, on June 23th 1980. She gained her diploma in mathematics from Beheshtian high school, Esfahan, Iran in 1999. Having a strong interest in physics, she started her bachelor program in applied physics at the Azad University, Shahreza, Iran and graduated in 2003. After that she followed her master program in atomic and molecular physics in Azad University, Tehran, Iran and graduated in 2007. In 2008 she started her PhD on the subject of "Validating the performance of a Raman laser spectrometer (RLS) instrument under Martian conditions" at the Petrology-Deep Earth and Planetary Science department. Five years of research have resulted in this thesis.